Available online at www.sciencedirect.com
ScienceDirect
Trans. Nonferrous Met. Soc. China 23(2013) 3476−3481
Transactions of Nonferrous Metals Society of China
www.tnmsc.cn

Si purification by enrichment of primary Si in Al−Si melt

Wen-zhou YU[1,2], Wen-hui MA[1,2], Guo-qiang LÜ[1], Yong-sheng REN[1,2], Hai-yang XUE[1], Yong-nian DAI[1,2]

1. Faculty of Metallurgical and Energy Engineering, Kunming University of Science and Technology, Kunming 650093, China;
2. National Engineering Laboratory for Vacuum Metallurgy, Kunming University of Science and Technology, Kunming 650093, China

Received 8 April 2013; accepted 3 July 2013

Abstract: The primary silicon crystals and Al−Si alloy in hypereutectic Al−Si melt were separated by electromagnetic stirring and directional solidification. Additionally, the distribution feature of impurities in Al−Si system was verified. The results show that the impurities are mainly located in Al−Si alloy and the grain boundaries between the Al−Si alloy and primary silicon. Furthermore, the morphology of primary silicon changes from fish-bone like to plate like and spheroid due to the different Si contents. The amount of impurities decreases with the increasing of Si content in different positions of the sample. The amount of impurities in the bottom of the sample is approximately 10×10^{-6}, which is obviously improved compared with the 1248.47×10^{-6} in metallurgical Si.
Key words: primary silicon; Al−Si alloy; electromagnetic stirring; directional solidification; impurity

1 Introduction

As the global economic crisis continues, worldwide businesses have been affected more or less, among which the photovoltaic (PV) industry is facing the problem of survival. Conventionally, the PV industry is seriously dependent on the expensive and off-spec semiconductor-grade silicon (SEG-Si) which leads to high cost of solar cells. To reduce the expense of raw materials, some low-cost fabrication routes of solar-grade silicon (SOG-Si) for PV industry should be proposed. In the last decades, metallurgical routes for SOG-Si preparation, which usually contain acid leaching [1], vacuum melting [2], oxidation treatment [3], slag refining [4], directional solidification [5,6] and electron beam melting [7], have been suggested to deal with the metallurgical grade silicon (MG-Si) by removing the impurities from it for the demand of SOG-Si, and it is considered a potential method for the cost reduction. Evidently, acid leaching can easily dissolve the impurities segregated in the grain boundaries of Si, and directional solidification is a well-known process for removing metallic impurities due to their strong segregation tendencies [8,9]. Additionally, for the removing of nonmetallic impurities, especially P and B, directional solidification may be ineffective due to the relatively large segregation coefficients (K_P=0.35, K_B=0.8) [10]. Therefore, vacuum melting and slag refining are always applied to remove P and B, respectively. Among the purification methods mentioned above, Si must be repeatedly molten in each step to ensure the impurities can easily transfer to outside, which may lead to a lot of energy consumption.

On the other hand, a new method named as “solvent refining” which can significantly cut down the temperature of melting, was proposed for further cost reduction of PV industry. YOSHIKAWA et al [11−13] and GU et al [14] proposed a Si−Al solvent to refine Si by the enhanced segregation tendency of impurities between solid silicon and the Si−Al melt. ZHAO et al [15] and MA et al [16] suggested a metal-liquating method using Sn−Si system which would have high efficiency for the removal of B. Additionally, Cu−Si [17] and Zn−Si [15] solvent refining methods were also related to the Si purification.

Overall, for the cost reduction of SOG-Si fabrication, the purification processes of MG-Si should be subject to principles as follows: 1) the temperature of

Foundation item: Project (u1137601) supported by the Joint Funds of the National Natural Science Foundation of China; Project (51066003) supported by the National Natural Science Foundation of China
Corresponding author: Wen-hui MA; Tel: +86-871-65161583; Fax: +86-871-65107208; E-mail: mwhsilicon@163.com
DOI: 10.1016/S1003-6326(13)62891-5

melting point for the raw materials must be low which can significantly cut down the energy consumption; 2) the process should be effective to remove most of impurities which contain metallic and nonmetallic instead of one single impurity; and 3) it should be environmental friendly which ensure all the final products be utilized rationally as much as possible.

For the purpose of energy conservation, a silicon purification method by separating the primary silicon from the Al−Si melt in hypereutectic Al−Si alloy system is proposed. The processes include: 1) the primary silicon crystals and Al−Si melt are separated by electromagnetic stirring in the induction furnace; 2) the impurities transfer from the primary silicon to Al−Si melt by segregation effect in directional solidification process; and 3) the product is cut apart along the separation interface between the primary silicon and Al−Si alloy, and then the primary silicon is cleaned by acid leaching to remove the residual Al attachment. In this work, the mass transferring characteristics of primary silicon crystals in the Al−Si melt due to the electromagnetic stirring is revealed, and the crystal growth mechanism is also discussed in detail. Furthermore, the distribution feature of impurities in Al−Si system is verified.

2 Experimental

The hypereutectic Al−45%Si (mass fraction) alloys were prepared firstly by the mixture of 36 g MG-Si powders and 44 g pure Al powders (99.99%), and then were melted to alloys in the electrical resistant-heating furnace. The MG-Si was leached by aqua regia (10%, 200 mL) for 2 h. After the leaching, the residues of silicon powders were thoroughly rinsed with deionized water until the solution was neutral, and then they were dried. The contents of main impurities in leached MG-Si were characterized by inductively coupled plasma mass spectrometry (ICP-MS), and the result is shown in Table 1.

Table 1 Impurity content in MG−Si (10^{-6})

Al	Fe	Ti	Ca	B	P
471	379	76.77	189	27.8	104.9

The separation process was carried out by placing the samples in the middle of coil zone of a 60 kW high frequency induction furnace, then heating the samples until they were completely molten. After being melted, the samples can be pulled down or up by the pulling system. The pulling rate was controlled at 19 μm/s, the temperature gradient was 25−31 °C/cm and the pulling distance was 8 cm away from the initial place. The argon gas was poured through the quartz tube to prevent the melt from being oxidized. The schematic diagram of the experiment equipment is shown in Fig. 1.

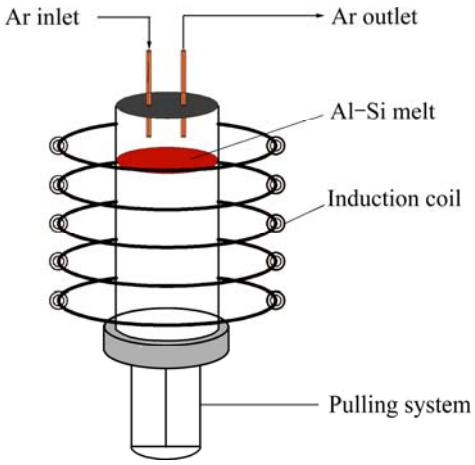

Fig. 1 Schematic diagram of experiment equipment

Then the solidified samples were cut apart from the separation interface between the precipitated primary silicon and the Al−Si alloy. To discuss the effect of purification, the primary silicon was firstly leached at the same conditions mentioned above to remove the residual Al attachment, and then it was characterized by ICP-MS, which can have a contrast with the result of MG-Si. The samples were polished to investigate the microstructure of primary silicon by an Olympus PME3 light optical microscopy (LOM) equipped with a KAPPA image analyzer. And the distribution of impurities in Al−Si system was verified by scanning electron microscope equipped with an energy dispersive spectrometer (SEM-EDS). The atomic absorption spectroscopy (AAS) was used to measure the Si content of different positions in the sample.

3 Results and discussion

3.1 Distribution of impurities in Al−Si alloy

It is well known that the impurities are subject to solid/liquid segregation during solidification of silicon from the Al−Si melt [10]. However, few reference has reported the distribution of impurities between the solidified silicon and the Al−Si melt. Figure 2 shows the distribution of impurities in Al−Si system.

From Fig. 2, it can be seen that the impurities such as C, O, Al, P and Ca tend to be located in Al−Si alloy, and Fe is apt to distribute in the grain boundaries between the primary silicon and Al−Si alloy. In addition, few impurities have been observed in primary silicon. It is clear that the impurities can be removed from the primary silicon during the solidification of primary silicon crystals from the Al−Si melt. However, for the purpose of Si purification in Al−Si system, the primary silicon and Al−Si alloy with most of impurities must be separated from each other.

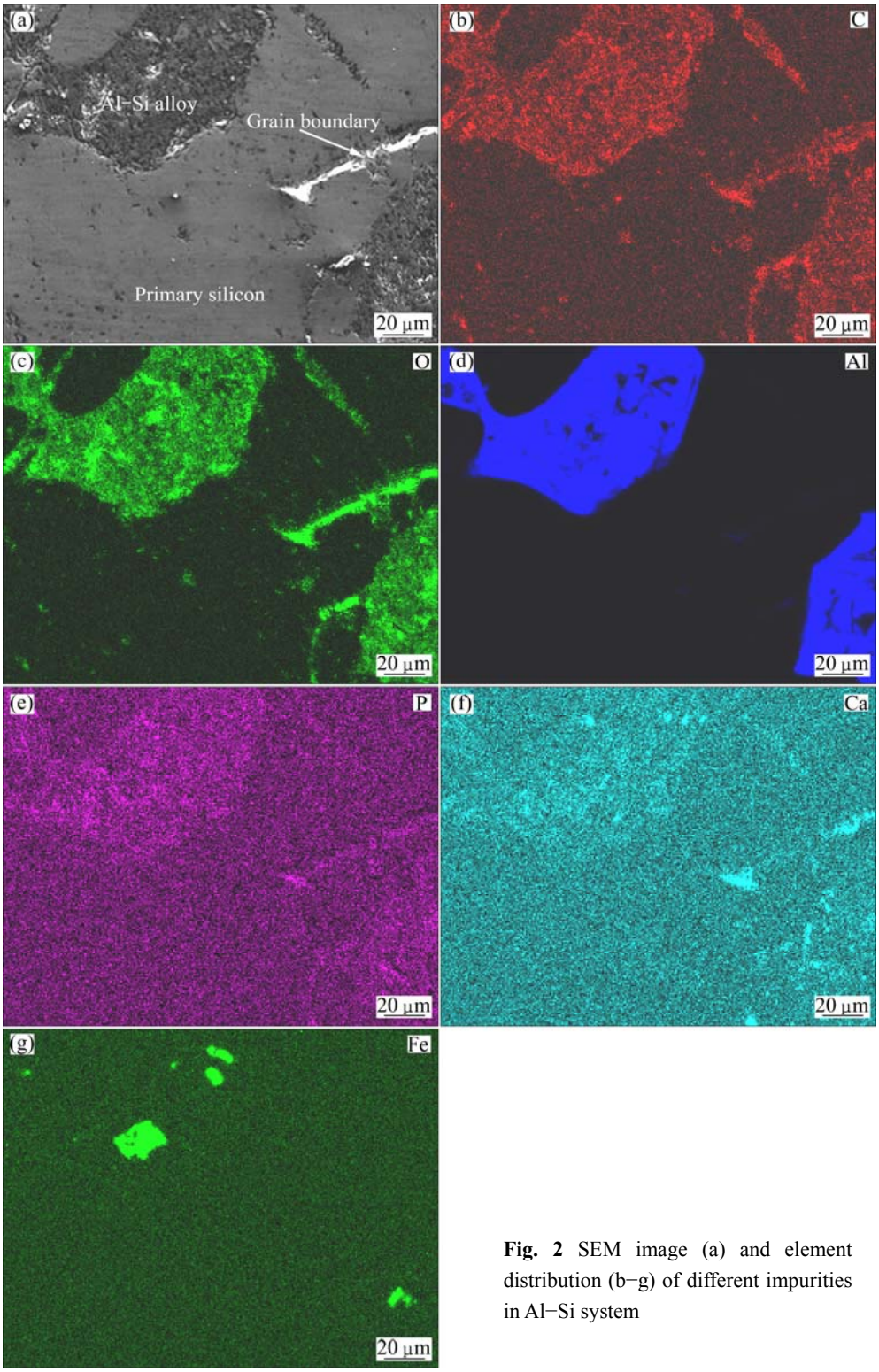

Fig. 2 SEM image (a) and element distribution (b−g) of different impurities in Al−Si system

3.2 Separation of primary silicon and Al−Si alloy

Figure 3 shows the cross-section morphologies of samples with and without the electromagnetic separation process.

It can be observed from Fig. 3(a) that the needle-like primary silicon distributes randomly in the Al−Si alloy when the electromagnetic field is absent. The reason is that the density of solid primary silicon is not much different from that of the Al−Si melt [18], which makes the primary silicon can't precipitate under the gravity force. From Figs. 3(b) and (c), it is easily found that the primary silicon precipitates at the lower part of the sample by pulling down. While pulling up, it precipitates at the upper part. This should be associated

with the fact that a melt flowing is formed in the Al−Si melt due to the electromagnetic stirring [13], thus the solidified primary silicon is carried downward or upward in the Al−Si melt. Meanwhile, a temperature gradient appears by pulling the sample down or up from the hot zone, which results in a viscosity gradient of the melt. When the primary silicon crystals are carried to the cold zone where the viscosity is high, they will precipitate at this zone. The simulation diagram about the movement of primary silicon in the Al−Si melt is shown in Fig. 4.

3.3 Morphologies of primary silicon

Figure 5 shows the microstructures of different positions in the sample. From Fig. 5(a), it can be seen that the morphology of the primary silicon near the separation interface between the primary silicon and Al−Si alloy is fish-bone shape. Figures. 5(b) and (c) show plate-like and spheroid morphologies of primary silicon respectively. The morphology of primary silicon has some relationships with the silicon content [19]. Figure 6 shows the silicon content of different positions in the sample. It is obviously recognized that the silicon content increases gradually from the top to the bottom.

This indicates that the morphology of primary silicon in the Al−Si melt is mainly decided by the silicon contents, and with the silicon content increasing, the morphology of primary silicon changes from fish-bone shape to plate-like, and then to spheroid, which is considered to be beneficial for the purification of silicon due to the low Al entrapment in this morphology [19]. The reason for the different Si content in different positions may be explained as follows. The precipitation of primary silicon mainly depends on electromagnetic stirring and viscosity gradient induced by the temperature gradient. According to the Al−Si binary diagram [20], the primary silicon continuously solidifies with the decreasing temperature. When the solidified primary silicon precipitates preferentially in the lower

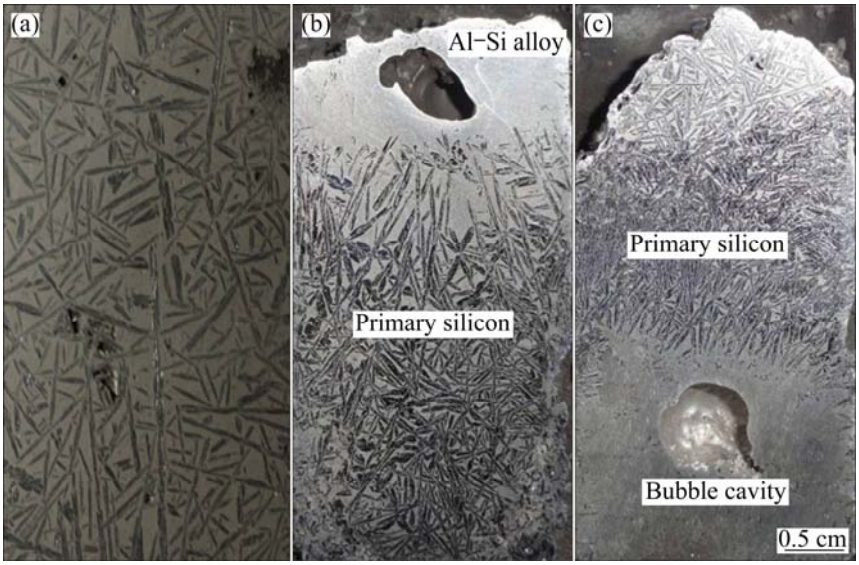

Fig. 3 Cross section morphologies of samples solidified under different conditions: (a) Without electromagnetic and pulling; (b) With pulling down and electromagnetic; (c) With pulling up and electromagnetic

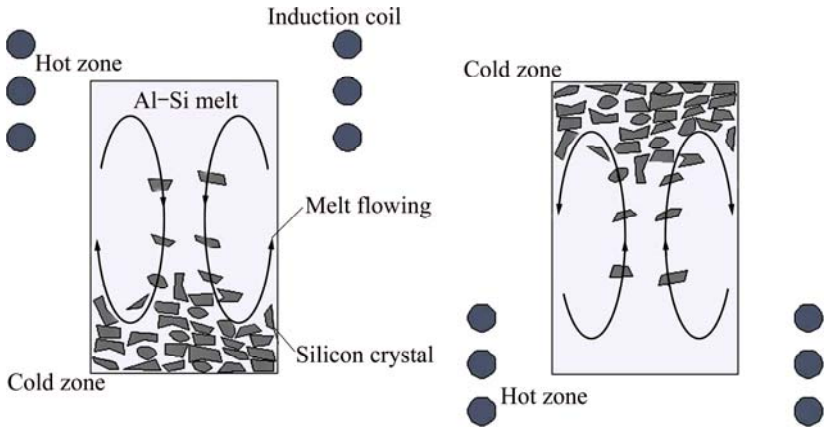

Fig. 4 Simulation diagram about movement of primary silicon in Al−Si melt

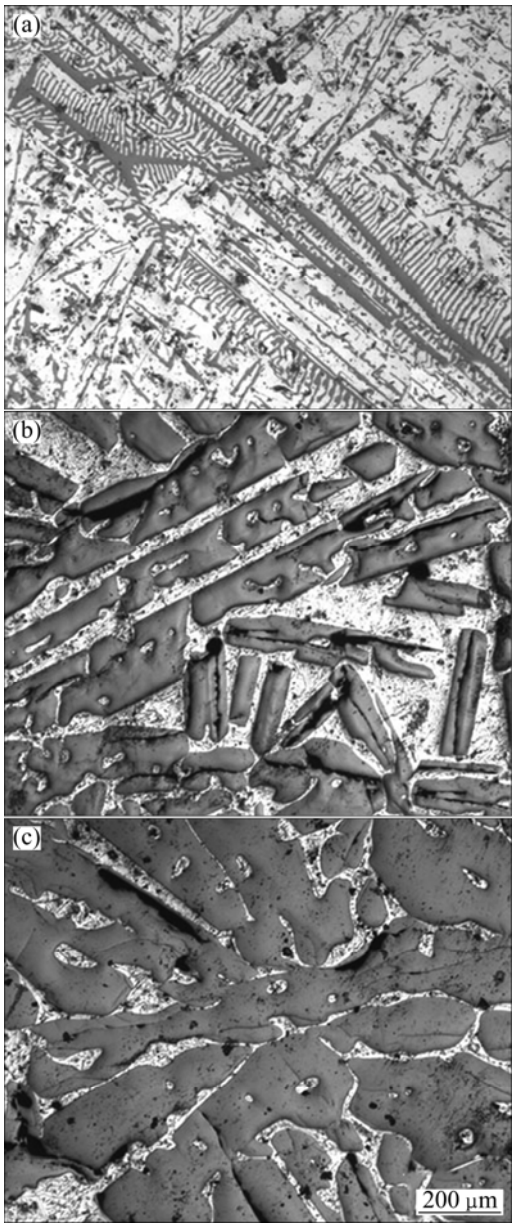

Fig. 5 Microstructures of primary silicon in different positions of sample: (a) Top part; (b) Middle part; (c) Bottom part

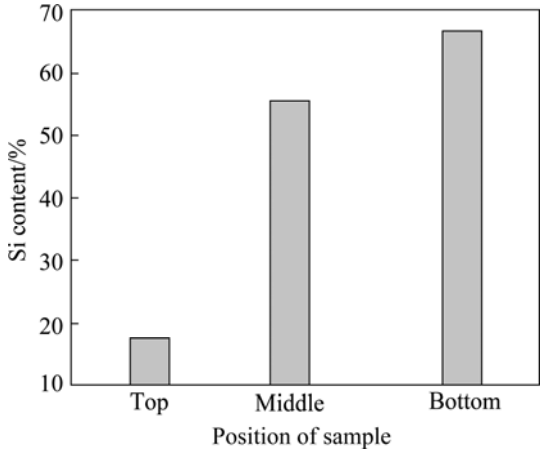

Fig. 6 Si content in different positions of sample

position during pulling down, the content of Si in Al−Si melt will decrease, thus the precipitation of primary silicon in upper position will correspondingly decrease.

Additionally, the impurity contents in different positions of the Si-rich zone, collected by acid leaching, are summarized in Fig. 7. It is obvious that with the silicon content increasing, the impurity contents decrease. The impurities content in the bottom position of the sample is approximately 10×10^{-6}, which is obviously improved compared with 1248.47×10^{-6} in metallurgical Si. This is because high Si content naturally brings on low Al content, and the spheroid morphology of Si also contains low Al entrapment. Furthermore, for the future work, it is best to promote the precipitation efficiency of primary silicon in all of the positions so that the morphology of primary silicon is spheroid, which will help to obtain Si of high-purity.

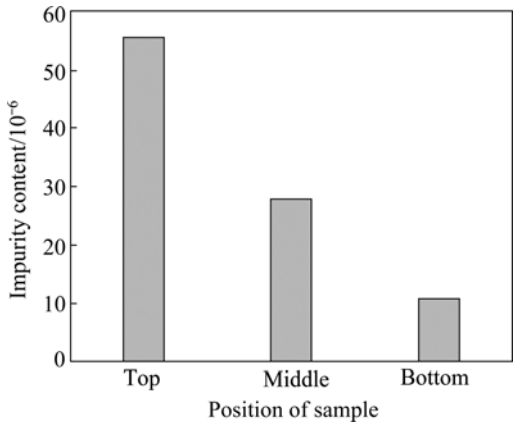

Fig. 7 Impurity contents in different positions of sample

4 Conclusions

1) The impurities are mainly located in Al−Si alloy and the boundaries between the Al−Si alloy and primary silicon.

2) The primary silicon crystals and Al−Si alloy have been separated from each other in the hypereutectic Al−Si melts by electromagnetic stirring and directional solidification.

3) The morphology of primary silicon changes from fish-bone like to plate like and spheroid due to different Si contents in different positions of silicon-rich part. And the impurities content decrease with the increasing of Si content in different positions of the sample. The impurities content in the bottom position of the sample is approximately 10×10^{-6}, which is obviously improved compared with the 1248.47×10^{-6} in metallurgical Si.

References

[1] DIETL J. Hydrometallurgical purification of metallurgical-grade silicon [J]. Solar Cells, 1983, 10(2): 145−154.

[2] WEI Kui-xian, MA Wen-hui, YANG Bin, LIU Da-chun, DAI Yong-nian, MORITA K. Study on volatilization rate of silicon in multicrystalline silicon preparation from metallurgical grade silicon [J]. Vacuum, 2011, 85(7): 749−754.
[3] NAKAMURA N, BABA H, SAKAGUCHI Y, KATO Y. Boron removal in molten silicon by a steam-added plasma melting method [J]. Materials Transactions, 2004, 45(3): 858−864.
[4] WU Ji-jun, MA Wen-hui, JIA Bin-jie, YANG Bin, LIU Da-chun, DAI Yong-nian. Boron removal from metallurgical grade silicon using a $CaO-Li_2O-SiO_2$ molten slag refining technique [J]. Journal of Non-Crystalline Solids, 2012, 358(23): 3079−3083.
[5] LIU L J, NAKANO S, KAKIMOTO K. Carbon concentration and particle precipitation during directional solidification of multicrystalline silicon for solar cells [J]. Journal of Crystal Growth, 2008, 310(7−9): 2192−2197.
[6] MARTORANO M A, FERREIRA NETO J B, OLIVEIRA T S, TSUBAKI T O. Refining of metallurgical silicon by directional solidification [J]. Materials Science and Engineering B, 2011, 176(3): 217−226.
[7] HANAZAWA K, YUGE N, KATO Y. Evaporation of phosphorus in molten silicon by an electron beam irradiation method [J]. Materials Transactions, 2004, 45(3): 844−849.
[8] HOPKINS R H, SEIDENSTICKER R G, DAVIS J R, RAI-CHOUDHURY P, BLAIS P D. Crystal growth considerations in the use of “solar grade” silicon [J]. Journal of Crystal Growth, 1977, 42: 493−498.
[9] NARUSHIMA T, YAMASHITA A, OUCHI C, IGUCHI Y. Solubilities and equilibrium distribution coefficients of oxygen and carbon in silicon [J]. Materials Transactions, 2002, 43(8): 2120−2124.
[10] TRUMBORE F A. Solid solubilities of impurity elements in germanium and silicon [J]. Bell System Technical Journal, 1960, 39: 205−233.
[11] MORITA K, YOSHIKAWA T. Thermodynamic evaluation of new metallurgical refining processes for SOG-silicon production [J]. Transactions of Nonferrous Metals Society of China, 2011, 21(3): 685−690.
[12] YOSHIKAWA T, ARIMURA K, MORITA K. Boron removal by titanium addition in solidification refining of silicon with Si−Al melt [J]. Metallurgical and Materials Transactions B, 2005, 36(6): 837−842.
[13] YOSHIKAWA T, MORITA K. Refining of silicon during its solidification from a Si−Al melt [J]. Journal of Crystal Growth, 2009, 311(3): 776−779.
[14] GU Xin, YU Xue-gong, YANG De-ren. Low-cost solar grade silicon purification process with Al−Si system using a powder metallurgy technique [J]. Separation and Purification Technology, 2011, 77(1): 33−39.
[15] ZHAO Li-xin, WANG Zhi, GUO Zhan-cheng, LI Cheng-yi. Low-temperature purification process of metallurgical silicon [J]. Transactions of Nonferrous Metals Society of China, 2011, 21(5): 1185−1192.
[16] MA X D, YOSHIKAWA T, MORITA K. Phase relations and thermodynamic property of boron in the silicon-tin melt at 1673 K [J]. Journal of Alloys and Compounds, 2012, 529: 12−16.
[17] MITRASINOVIC A M, UTIGARD T A. Refining silicon for solar cell application by copper alloying [J]. Silicon, 2009, 1(4): 239−248.
[18] MAGNUSSON T, ARNBERG L. Density and solidification shrinkage of hypoeutectic aluminum-silicon alloys [J]. Metallurgical and Materials Transactions A, 2001, 32(10): 2605−2613.
[19] ULLAH M W, CARLBERG T. Silicon crystal morphologies during solidification refining from Al−Si melts [J]. Journal of Crystal Growth, 2011, 318(1): 212−218.
[20] MURRAY J L, MCALISTER A J. The Al−Si (Aluminum-Silicon) system [J]. Bulletin of Alloy Phase Diagrams, 1984, 5(1): 74−84.

铝硅熔体中富集初晶硅提纯硅

余文轴[1,2]，马文会[1,2]，吕国强[1]，任永生[1,2]，薛海洋[1]，戴永年[1,2]

1. 昆明理工大学 冶金与能源工程学院，昆明 650093；
2. 昆明理工大学 真空冶金国家工程实验室，昆明 650093

摘　要：采用电磁搅拌结合定向凝固技术将过共晶铝硅合金中的初晶硅和铝硅合金分离，并研究不同的杂质元素在铝硅体系中的分布特点。结果表明：杂质元素主要分布在铝硅合金以及铝硅合金和初晶硅的晶界中。同时，根据初晶硅富集区域不同位置硅含量的不同，初晶硅的形貌由鱼骨状变成板状和球状，并且随着样品中不同位置硅含量的增多，初晶硅中的杂质含量降低。样品底部杂质的含量约为 10×10^{-6}，与原料冶金级硅中的杂质含量 1248.47×10^{-6} 相比，杂质的去除效果很好。

关键词：初晶硅；铝硅合金；电磁搅拌；定向凝固；杂质

(Edited by Chao WANG)